Electronic Supplementary Material (ESI) for Environmental Science: Nano.


# Supporting Information

# Photocatalytic Reduction of Cr(VI) by Graphene Oxide Materials under Sunlight or Visible Light: the Effects of Low-Molecular-Weight Chemicals

*Shang-Shing Wu [†], Wen-Che Hou[*,†] David K. Wang[‡]*

[†]*Department of Environmental Engineering, National Cheng Kung University, Tainan City, Taiwan, 70101*

[‡]*School of Chemical and Biomolecular Engineering, the University of Sydney, Darlington, New South Wales, 2006, Australia*

**Address correspondence to Wen-Che Hou: Phone: +886 62757575 ext.65842, Fax: +886 6 2752790, E-mail: whou@mail.ncku.edu.tw*

**Manuscript prepared for publication in:**

**Pages: 18**

**Figures: S1-6**

**Table: S1**

**GO synthesis.** A mixture of $H_2SO_4/H_3PO_4$ at a ratio of 9:1 v/v, (i.e., 360:40 mL) was slowly added to a mixture of graphite flakes (3.0 g) and $KMnO_4$ (18.0 g) in an Erlenmeyer flask (1000 mL). The sample temperature was slightly increased to 30$^{o}$C during the slow acid addition. The mixture was stirred and allowed to incubate at 50$^{o}$C for 12 h in a water bath heated on a hot plate. The sample was then transferred to an ice water bath. A solution of water (400 mL) and 30% $H_2O_2$ (w/w, 3 mL) was added to the sample that was incubated for 30 min. The oxidized graphite flakes were collected by centrifugation (3000 g, 10 min) and the precipitate was re-suspended in 10 % HCl (v/v) and centrifuged again. The re-suspension and centrifugation steps were repeated 3 times. Subsequently, the sample was rinsed with pure water by repeated centrifugation (8000 g, 30 min) and re-suspension in pure water until the pH became constant (~5.0). The oxidized graphite sample was lyophilized (FD-4.5, KINGMECH, Taiwan). About 6.0 g of oxidized graphite powders could be obtained and was stored in the dark at room temperature. Prior to use, 1,000 mg of oxidized graphite sample was added to 1 L of pure water and exfoliated in a cleaner-type of sonicator for 60 min to obtain GO.

**rGO synthesis.** GO was reduced by ascorbic acid to rGO.[1] Briefly, 100 mg/L GO was mixed with 0.1 M ascorbic acid and then the mixture was allowed to react at 80$^{o}$C for 24 h. Afterwards, the rGO material was collected on 0.45 μm filtration membranes. The rGO material was then re-dispersed in DI water. The procedure was repeated 4 times to remove residual chemicals (e.g., ascorbic acid and byproducts). The rGO sample was then lyophilized to obtain rGO powders.

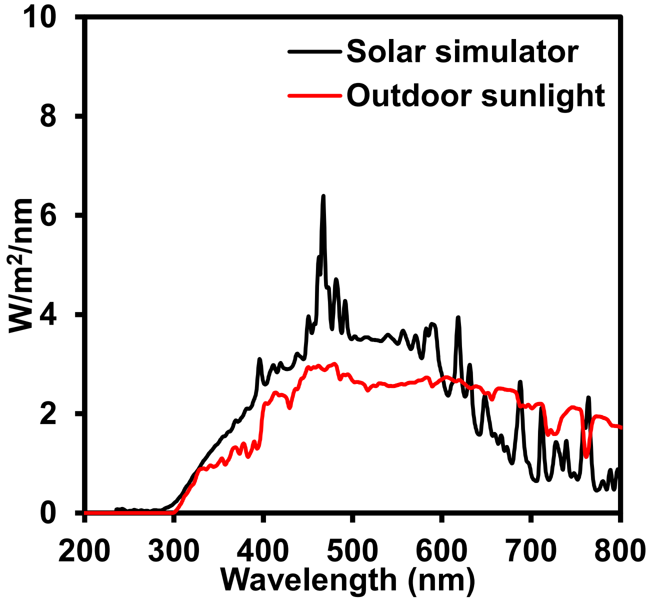


**Figure S1.** Spectra of solar simulator sunlight and outdoor summer noon sunlight in a clear day in Tainan, Taiwan (23°0'0.44" N, 120°13'18.1" E).[2]

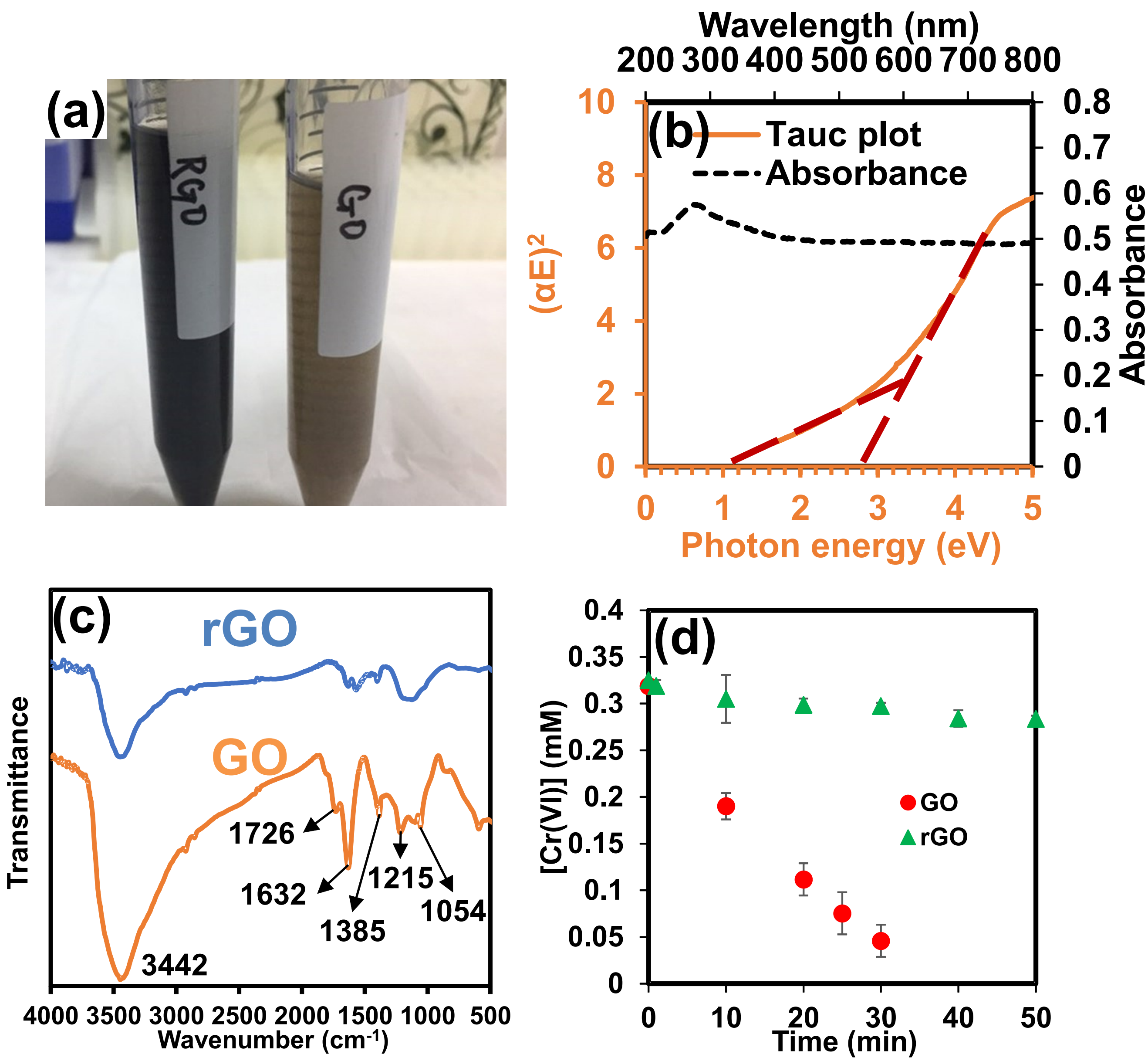


**Figure S2.** (a) Image of GO and rGO, (b) the absorbance spectrum and Tauc plot of rGO, (c) the FTIR spectra of GO and rGO, and (d) the photocatalytic reduction of Cr(VI) by rGO under solar irradiation. Condition: [rGO] = 200 mg/L, [oxalate] = 20 mM, [Cr(VI)] = 0.32 mM, pH = 3.0. The error bars indicate ± one standard deviation from triplicate samples. The Cr(VI) concentrations of rGO samples already account for the dark control experiment by subtracting the lost Cr(VI) concentrations in corresponding dark control samples. The GO data that are used for comparison are those presented in Figure 3.

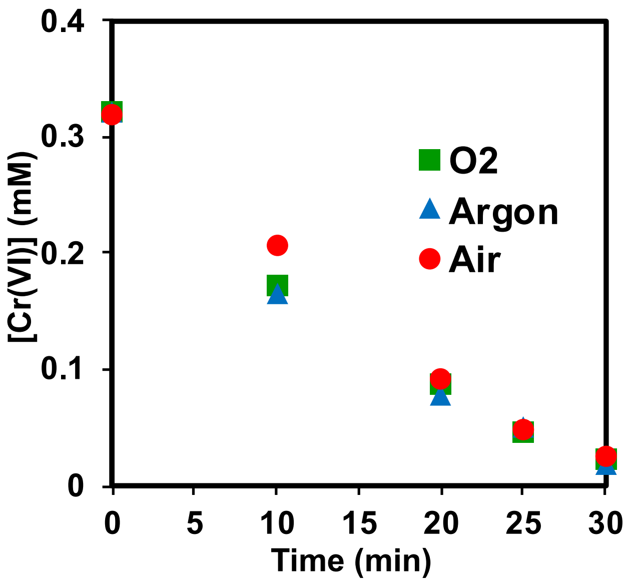


**Figure S3.** Photocatalytic reduction of Cr(VI) by GO in air-equilibrated, argon- or $O_2$-bubbled experiments under solar irradiation. Condition: [GO] = 200 mg/L, [oxalate] = 20 mM, pH = 3.0.

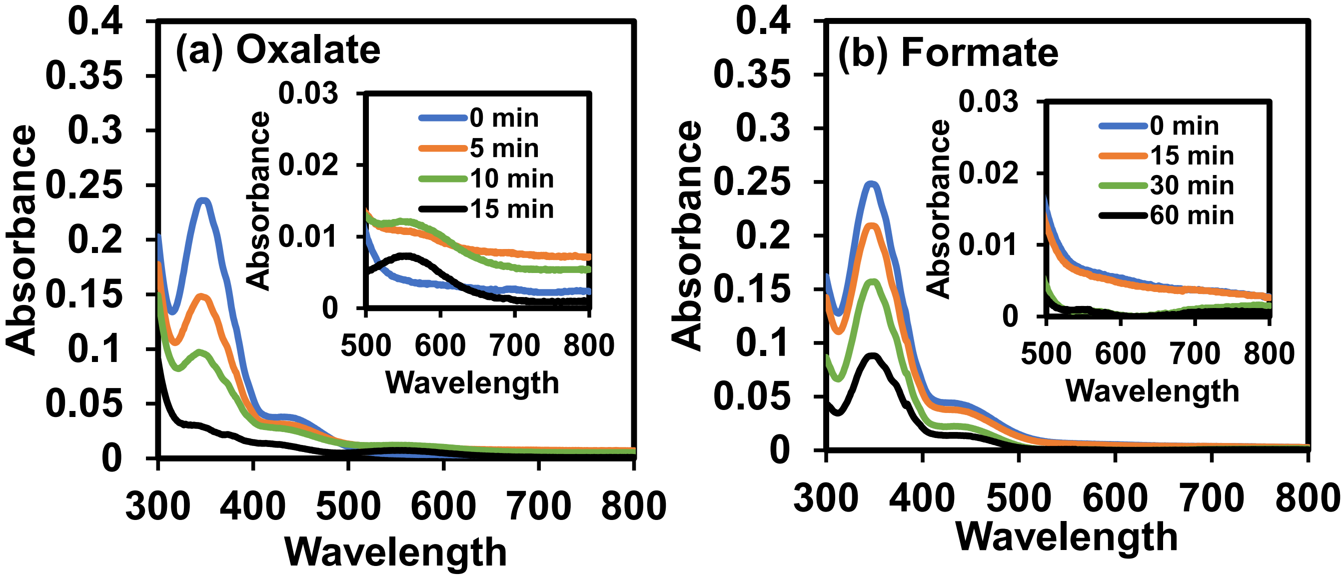


**Figure S4.** UV-visible absorbance spectra of samples during photoreduction of Cr(VI) in the presence of (a) oxalate, or (b) formate under sunlight irradiation. Condition: [Cr(VI)] = 0.16 mM, [Oxalate] or [Formate] = 20 mM, [GO] = 200 mg/L, pH = 3.0. The UV-visible spectra were recorded immediately upon sampling after passing through 0.22-μm PTFE filters to remove GO.

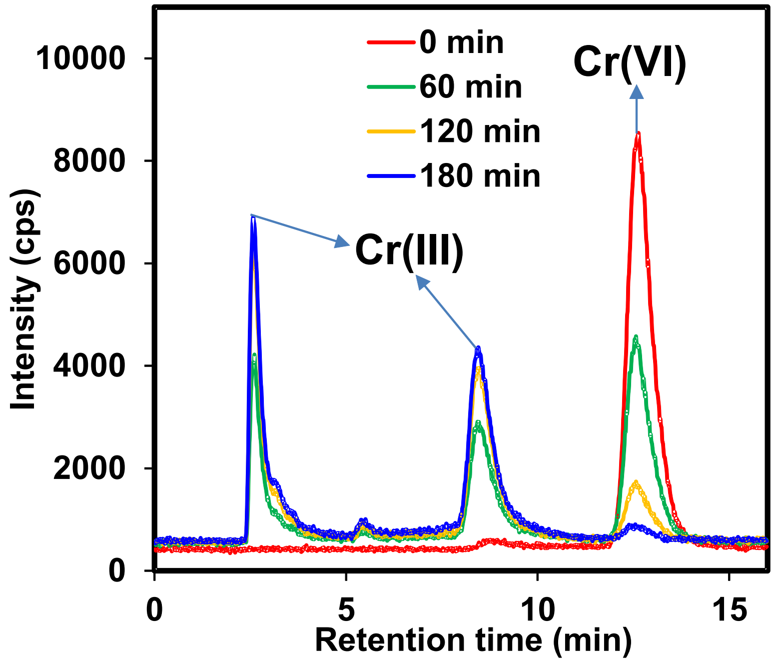


**Figure S5.** HPLC chromatogram showing the speciation of Cr during photoreaction. The photoreaction condition: [GO] = 200 mg/L, [oxalate] = 1 mM, pH = 3.0, $[Cr(VI)]_0$ = 0.32 mM.

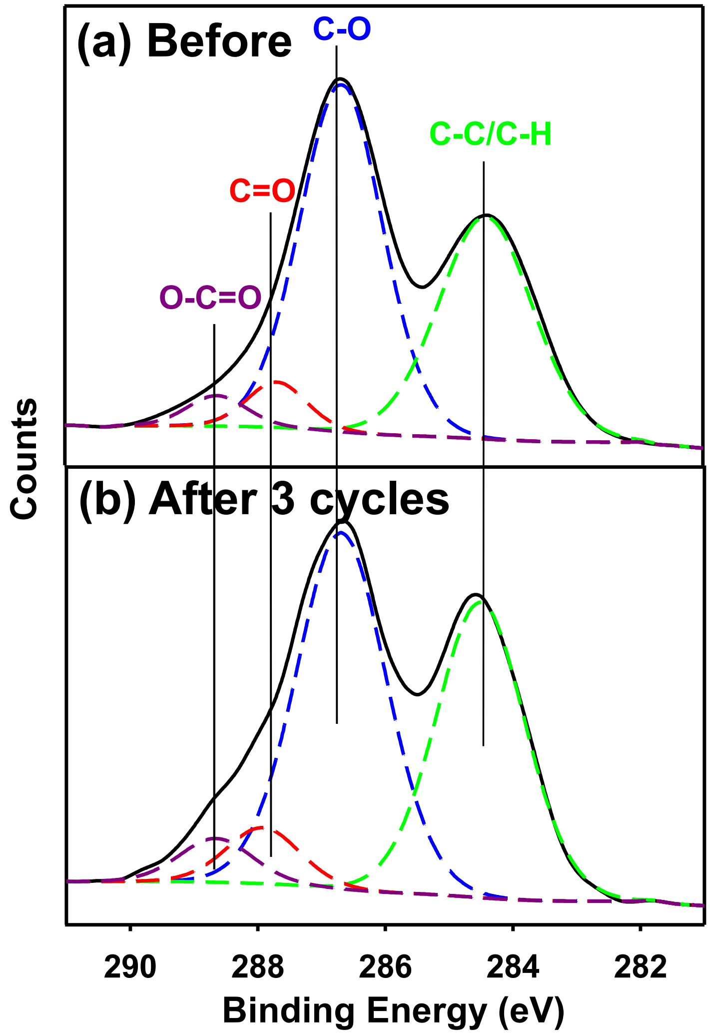


| Sample | O:C | C-C/C-H% | C-O% | C=O% | O-C=O% |
|---|---|---|---|---|---|
| Before | 0.51 | 38.7 | 53.0 | 5.0 | 3.3 |
| After 3 cycles | 0.44 | 40.1 | 48.8 | 6.2 | 4.9 |

**Figure S6.** XPS spectra showing the oxygen-to-carbon ratio (O:C) and functionality changes of GO (a) before, and (b) after 3 cycles of photoreaction under visible light irradiation. Condition: [GO] = 200 mg/L, [Cr(VI)] = 0.32 mM, [oxalate] = 20 mM, pH = 3.0. Used GO was dialyzed (3 KDa MWCO UF membrane) against DI water to remove residual chemicals (e.g., Cr, oxalate, etc.) before XPS analysis.

**Table S1.** Summary of studies using carbon-based nanomaterials in photocatalytic reduction of Cr(VI)

| Photocatalyst | Catalyst dose (g/L) | Light source | Organic electron donor | pH | [Cr(VI)] reduction | Δ[Cr(VI)]/Δt /[catalyst] (mM $h^{-1}$ L $g^{-1}$) | Ref. |
|---|---|---|---|---|---|---|---|
| GO | 0.2 | Simulated sunlight | None | 3 | 0.11 mM in 2 h | **0.285** | This work |
| GO | 0.2 | Simulated sunlight | Oxalate | 3 | 0.27 mM in 0.5 h | **2.730** | This work |
| GO | 0.2 | Visible light, > 400 nm | Oxalate | 3 | 0.18 mM in 0.5 h | **1.820** | This work |
| GO | 0.05 | Simulated sunlight | None | 3 | 0.11 mM in 2 h | **1.100** | This work |
| GO | 0.05 | Simulated sunlight | Oxalate | 3 | 0.30 mM in 0.67 h | **8.955** | This work |
| rGO/$TiO_2$ composite | 1 | 500 W Hg lamp | None | NA* | 0.17 mM in 4 h | 0.043 | Liu et al., RSC Advances, 2011.[3] |
| rGO/$TiO_2$ composite | 0.2 | 125 W Hg lamp, > 450 nm | None | 2.6 | 0.14 mM in 4 h | 0.173 | Zhao et al., J. Colloid and Interface Science, 2013.[44] |
| Carbon dot/$TiO_2$ composite | 1 | 365 nm UV LED light | None | 3 | 0.12 mM in 0.5 h | 0.230 | Zhang et al., Applied Catalyst B-Environmental, 2018.[5] |
| Graphene hydrogel/$TiO_2$ composite | 1 | 250 W Hg lamp, 365 nm | None | 5.5 | 0.10 mM in 0.5 h | 0.192 | Li et al., Applied Catalyst B-Environmental, 2016.[6] |
| rGO/$TiO_2$ microspheres composite | 0.67 | 300 W Xe lamp, > 400 nm | None | 3 | 0.15 mM in 3 h | 0.077 | Liu et al., J. Alloys and Compounds, 2017.[7] |
| rGO/$TiO_2$ composite | 0.8 | 125 W Hg lamp | None | 2 | 0.31 mM in 3.5 h | 0.110 | Shaikh et al., J. Nanoparticles Research, 2017.[8] |
| rGO/ZnO composite | 1 | 500 W Hg lamp | None | NA | 0.19 mM in 4 h | 0.048 | Liu et al., Catalysis Science & Technology, 2011.[9] |
| rGO/ZnO composite | 1 | 500 W Hg lamp | None | NA | 0.18 mM in 1 h | 0.184 | Liu et al., Chemical Engineering J., 2012.[10] |
| rGO/ZnO composite | 0.25 | 300 W Xe lamp, 365 nm | None | NA | 0.07 mM in 1.3 h | 0.200 | Zhang et al., Applied Catalyst |

| | | | | | | | |
|---|---|---|---|---|---|---|---|
| | | | | | | | B-Environmental, 2013.[11] |
| rGO/CdS composite | 1 | 400-W halogen lamp, > 400 nm | None | NA | 0.17 mM in 4 h | 0.043 | Liu et al., Chemical Communications, 2011.[12] |
| rGO/UiO-66(NH2) composite | 0.5 | 300-W Xe arc lamp, > 420 nm | None | 2 | 0.19 mM in 1.7 h | 0.230 | Shen et al., RSC Advances, 2014.[13] |
| Graphene/hematite composites | 1 | 300 W Xe lamp, > 420 nm | None | 2 | 0.18 mM in 2.7 h | 0.066 | Du et al., RSC Advances, 2015.[14] |
| GO/coordination polymer nanobelt composite | 0.25 | 300 W Xe lamp, ≥ 420 nm | None | NA | 0.05 mM in 3.3 h | 0.065 | Shi et al., Dalton Trans., 2015.[15] |
| rGO/magnetic $Fe_3O_4$ composite | 0.5 | Sunlight | None | 3 | 0.06 mM in 0.5 h | 0.240 | Boruah et al., RSC Advances, 2016.[16] |
| GO, doped with Fe(III) | 0.04 | 500 W halogen lamp, > 420 nm | None | 3 | 0.04 mM in 1 h | 1.0 | Liu et al., Scientific Report, 2017.[17] |
| Graphene/$Ni_3S_2$ composite | 1 | 300 W Xe lamp, > 400 nm | None | NA | 0.35 mM in 3 h | 0.117 | Hu et al., J. Colloid and Interface Science, 2017.[18] |
| Graphene/$Nb_2O_5$ nanorods composite | 1 | 300 W Xe lamp, > 420 nm | 4-chlorophenol | 3 | 0.17 mM in 4 h | 0.043 | Yang et al., Chemical Engineering J., 2018.[19] |
| rGO/ZnAlTi double oxide composite | 0.4 | 30 W LED lamp | None | 3 | 0.05 mM in 3 h | 0.040 | Ye et al., Chemosphere, 2019.[20] |
| rGO functionalized/CuS composite | 0.4 | Sunlight | Glucose | 3 | 0.08 mM in 0.4 h | 0.452 | Borthakur et al., ACS Sustainable Chem. Engr., 2019.[21] |
| rGO/Ag/$Ag_3PO_4$ microspheres | 1 | 210 W Xe lamp, > 400 nm | Lactic acid | 5 | 0.12 mM in 0.5 h | 0.230 | Liu et al., Chemical Engr. J., 2020.[22] |
| g-$C_3N_4$/ZnO composite | 2 | 500 W Xe lamp, > 400 nm | None | NA | 0.05 mM in 1.67 h | 0.014 | Liu et al., Chemical Engr. J., 2012.[23] |

| | | | | | | | |
|---|---|---|---|---|---|---|---|
| g-$C_3N_4$, formate modified | 1 | 300 W Xe lamp, > 420 nm | Formate | NA | 0.19 mM in 4 h | 0.048 | Dong et al., J. Phys. Chem. C, 2013.[24] |
| g-$C_3N_4$ | 1 | 300 W Xe lamp, > 420 nm | Trichlorophenol | 3 | 0.095 mM in 2 h | 0.048 | Hu et al., Catalysis Today, 2014.[25] |
| g-$C_3N_4$ | 1 | 250 W Xe lamp, > 420 nm | Citric acid | 3.2 | 0.34 mM in 5 h | 0.068 | Zhang et al., Separation and Purification Technol., 2015.[26] |
| g-$C_3N_4$, acid-treated | 1 | 250 W Xe lamp, > 420 nm | Citric acid | 3.2 | 0.34 mM in 3.5 h | 0.097 | Zhang et al., Separation and Purification Technol., 2015.[26] |
| g-$C_3N_4$/α-$Fe_2O_3$ composite | 2 | 300 W Xe lamp, > 400 nm | None | 2 | 0.19 mM in 2.5 h | 0.038 | Xiao et al., Applied Surface Science, 2015.[27] |
| g-$C_3N_4$/$Ti^{3+}$-$TiO_2$ composite | 1 | 300 W Dy lamp, > 400 nm | None | 2 | 0.14 mM in 2 h | 0.068 | Lu et al., Applied Surface Science, 2015.[28] |
| g-$C_3N_4$, $HNO^{3-}$ treated | 1 | 250 W Xe lamp, > 420 nm | Citric acid | 3.1 | 0.07 mM in 2.5 h | 0.027 | Wei et al., Applied Catalysis A-General, 2016.[29] |
| g-$C_3N_4$/$TiO_2$ composite | 1 | 300 W Xe lamp, > 420 nm | None | 3 | 0.095 mM in 4 h | 0.024 | Mohini et al., Materials Research Bulletin, 2016.[30] |
| g-$C_3N_4$/MIL-53(Fe) composite | 0.4 | 500 W Xe lamp, > 420 nm | None | 3 | 0.18 mM in 3 h | 0.148 | Huang et al., Applied Surface Science, 2017.[31] |
| g-$C_3N_4$, sulfur doped | 0.25 | 300 W Xe lamp, > 400 nm | Oxalate | NA | 0.096 mM in 0.5 h | 0.768 | Zheng et al., Molecules, 2017.[32] |
| g-$C_3N_4$, loaded on TiSBA15 | 1 | 300 W Xe lamp, > 420 nm | None | 2.3 | 0.14 mM in 5 h | 0.028 | Liu et al., Applied catalysis B-Environmental, 2017.[33] |
| g-$C_3N_4$/$Bi_{12}GeO_{20}$ composite | 3 | 300 W Dy lamp, > 400 nm | None | 2.5 | 0.19 mM in 3 h | 0.021 | Wan et al., Applied Catalysis B-Environmental, 2017.[34] |

| | | | | | | | |
|---|---|---|---|---|---|---|---|
| $g-C_3N_4$, Mn doped and carboxylated | 0.5 | 300 W Xe lamp, > 400 nm | None | NA | 0.10 mM in 1 h | 0.200 | Wang et al., J. Hazardous Materials, 2017.[35] |
| $g-C_3N_4/SnS_2/SnO_2$ composites | 0.5 | 300 W Xe lamp, > 400 nm | Ethanol | 2.1 | 0.35 mM in 1 h | 0.728 | Yang et al., Chemical Engr. J., 2018.[36] |
| $g-C_3N_4$/charcoal composite | 1 | 30 W LED lamp, > 420 nm | None | 3 | 0.018 mM in 3 h | 0.006 | Lamkhao et al., Chemosphere, 2018.[37] |
| $g-C_3N_4$, phosphorus doped | 1 | 300 W Xe lamp, > 400 nm | Dichlorophenol | 2.13 | 0.39 mM in 1 h | 0.385 | Deng et al., Applied Catalysis B-Environmental, 2018.[38] |
| $g-C_3N_4/Ag@Ag_3PO_4$/ NiFe LDH composite | 1 | Simulated sunlight | None | 5 | 0.31 mM in 2 h | 0.154 | Nayak et al., ACS Omega, 2018.[39] |
| $g-C_3N_4$/Au nanoparticle composite | 0.2 | 300 W Xe lamp, > 400 nm | None | 3 | 0.154 mM in 2 h | 0.385 | Chang et al., J. Hazardous Materials, 2018.[40] |
| $g-C_3N_4/GO/BiFeO_3$ composite | 2.5 | 300 W Xe lamp, > 400 nm | None | 2 | 0.07 mM in 1.3 h | 0.020 | Hu et al., Chemosphere, 2019.[41] |
| $g-C_3N_4$ | 1.1 | 300 W Xe lamp | None | NA | 0.34 mM in 4.5 h | 0.069 | Hu et al., Polymer, 2019.[42] |
| $g-C_3N_4$/HCl or phytic acid-doped PANI composite | 1.1 | 350 W Xe lamp | None | NA | 0.27 mM in 0.17 h | 1.455 | Wu et al, ACS Applied Materials Interfaces, 2019.[43] |
| $g-C_3N_4/Ag/Bi_4O_7$ composite | 0.3 | 300 W Xe lamp, > 420 nm | None | 3 | 0.34 mM in 0.83 h | 1.365 | Ye et al., J. Hazardous Materials, 2019.[44] |
| $g-C_3N_4$/palygorskite composite | 0.5 | 300 W Xe lamp, > 400 nm | None | 2 | 0.68 mM in 1.67 h | 0.814 | Zhang et al., Chemical Engr. J., 2019.[45] |
| $g-C_3N_4$/UiO-66 composite | 0.5 | 300 W Xe lamp | None | 2 | 0.17 mM in 0.67 h | 0.516 | Yi et al., Chemical Engr. J., 2019.[46] |
| $g-C_3N_4$, ammonia plasma modified | 0.4 | 500 W Xe lamp, > 420 nm | None | NA | 0.75 mM in 2 h | 0.933 | Kang et al., ACS Applied Materials Interfaces, 2019.[47] |
| $g-C_3N_4$, made under N2 atmosphere | NA | 300 W Xe lamp, > 420 nm | Bisphenol A | 3.5 | 0.18 mM in 2 h | NA | Wang et al., Catalysis Today, |

| | | | | | | | |
|---|---|---|---|---|---|---|---|
| | | | | | | | 2019.[48] |
| g-$C_3N_4$/$TaC_xO_y$ composite | 1 | 500 W Xe lamp, > 420 nm | Citric acid | NA | 0.33 mM in 0.58 h | 0.564 | Zhang et al., Catalysis Communications, 2019.[49] |
| g-$C_3N_4$/ZnS composite | 0.8 | 500 W Xe lamp, > 420 nm | None | NA | 0.18 mM in 2 h | 0.109 | Wang et al., Applied Surface Science, 2019.[50] |
| g-$C_3N_4$/N doped $TiO_2$/diatomite composite | 2 | 500 W Xe lamp, > 400 nm | Glucose | 2 | 0.08 mM in 4 h | 0.010 | Sun et al., Environmental Pollution, 2019.[51] |
| g-$C_3N_4$, B doped/$BiVO_4$ composite | 2.5 | 150 W Xe lamp, > 420 nm | None | 2 | 0.33 mM in 0.5 h | 0.262 | Babu et al., Inorganic Chemistry, 2019.[52] |
| g-$C_3N_4$, hydroxyl modified | 1 | 300 W Xe lamp | None | 2.3 | 0.39 mM in 0.75 h | 0.513 | Wang et al., Applied Surface Science, 2020.[53] |
| g-$C_3N_4$, sulfonic acid modified | 0.5 | 300 W Xe lamp, >400 nm | Citric acid | 2 | 0.16 mM in 0.67 h | 0.487 | Meng et al., Materials Research Bulletin, 2020.[54] |
| g-$C_3N_4$/biochar composite | 40 | 300 W Xe lamp, > 400 nm | None | 2 | 0.48 mM in 4 h | 0.003 | Jin et al., RSC Advances, 2020.[55] |
| N-doped carbon | 0.4 | 500 W Xe lamp, > 420 nm | None | 2 | 0.43 mM in 3.5 h | 0.309 | Li et al., Science of the Total Environment, 2020.[56] |

*NA: not available

## References


1 C. Chen, Y.-C. Chen, Y.-T. Hong, T.-W. Lee and J.-F. Huang, Facile fabrication of ascorbic acid reduced graphene oxide-modified electrodes toward electroanalytical determination of sulfamethoxazole in aqueous environments, *Chemical Engineering Journal*, 2018, **352**, 188–197.

2 W.-C. Hou and S.-H. Huang, Photochemical reactivity of aqueous fullerene clusters: C60 versus C70, *Journal of Hazardous Materials*, 2017, **322, Part A**, 310–317.

3 X. Liu, L. Pan, T. Lv, G. Zhu, T. Lu, Z. Sun and C. Sun, Microwave-assisted synthesis of TiO2-reduced graphene oxide composites for the photocatalytic reduction of Cr(VI), *RSC Adv.*, 2011, **1**, 1245–1249.

4 Y. Zhao, D. Zhao, C. Chen and X. Wang, Enhanced photo-reduction and removal of Cr(VI) on reduced graphene oxide decorated with TiO2 nanoparticles, *Journal of Colloid and Interface Science*, 2013, **405**, 211–217.

5 Y. Zhang, M. Xu, H. Li, H. Ge and Z. Bian, The enhanced photoreduction of Cr(VI) to Cr(III) using carbon dots coupled TiO2 mesocrystals, *Applied Catalysis B: Environmental*, 2018, **226**, 213–219.

6 Y. Li, W. Cui, L. Liu, R. Zong, W. Yao, Y. Liang and Y. Zhu, Removal of Cr(VI) by 3D TiO2-graphene hydrogel via adsorption enriched with photocatalytic reduction, *Applied Catalysis B: Environmental*, 2016, **199**, 412–423.

7 L. Liu, C. Luo, J. Xiong, Z. Yang, Y. Zhang, Y. Cai and H. Gu, Reduced graphene oxide (rGO) decorated TiO2 microspheres for visible-light photocatalytic reduction of Cr(VI), *Journal of Alloys and Compounds*, 2017, **690**, 771–776.

8 A. Shaikh, S. P. Mishra, P. Mohapatra and S. Parida, One-step solvothermal synthesis of TiO2-reduced graphene oxide nanocomposites with enhanced visible light photoreduction of Cr(VI), *J Nanopart Res*, 2017, **19**, 206.

9 X. Liu, L. Pan, T. Lv, T. Lu, G. Zhu, Z. Sun and C. Sun, Microwave-assisted synthesis of ZnO–graphene composite for photocatalytic reduction of Cr( vi ), *Catalysis Science & Technology*, 2011, **1**, 1189–1193.

10 X. Liu, L. Pan, Q. Zhao, T. Lv, G. Zhu, T. Chen, T. Lu, Z. Sun and C. Sun, UV-assisted photocatalytic synthesis of ZnO–reduced graphene oxide composites with enhanced photocatalytic activity in reduction of Cr(VI), *Chemical Engineering Journal*, 2012, **183**, 238–243.

11 Y. Zhang, Z. Chen, S. Liu and Y.-J. Xu, Size effect induced activity enhancement and anti-photocorrosion of reduced graphene oxide/ZnO composites for degradation of organic dyes and reduction of Cr(VI) in water, *Applied Catalysis B: Environmental*, 2013, **140–141**, 598–607.

12 X. Liu, L. Pan, T. Lv, G. Zhu, Z. Sun and C. Sun, Microwave-assisted synthesis of CdS–reduced graphene oxide composites for photocatalytic reduction of Cr(VI), *Chem. Commun.*, 2011, **47**, 11984–11986.

13 L. Shen, L. Huang, S. Liang, R. Liang, N. Qin and L. Wu, Electrostatically derived self-assembly of NH2-mediated zirconium MOFs with graphene for photocatalytic reduction of Cr(VI), *RSC Adv.*, 2013, **4**, 2546–2549.

14 Y. Du, Z. Tao, J. Guan, Z. Sun, W. Zeng, P. Wen, K. Ni, J. Ye, S. Yang, P. Du and Y. Zhu, Microwave-assisted synthesis of hematite/activated graphene composites with superior performance for photocatalytic reduction of Cr(VI), *RSC Adv.*, 2015, **5**, 81438–81444.

15 G.-M. Shi, B. Zhang, X.-X. Xu and Y.-H. Fu, Graphene oxide coated coordination polymer nanobelt composite material: a new type of visible light active and highly efficient photocatalyst for Cr( vi ) reduction, *Dalton Transactions*, 2015, **44**, 11155–11164.

16 P. K. Boruah, P. Borthakur, G. Darabdhara, C. K. Kamaja, I. Karbhal, M. V. Shelke, P. Phukan, D. Saikia and M. R. Das, Sunlight assisted degradation of dye molecules and reduction of toxic Cr(VI) in aqueous medium using magnetically recoverable Fe3O4/reduced graphene oxide nanocomposite, *RSC Adv.*, 2016, **6**, 11049–11063.

17 R. Liu, X. Zhu and B. Chen, A New Insight of Graphene oxide-Fe(III) Complex Photochemical Behaviors under Visible Light Irradiation, *Sci Rep*, 2017, **7**, 1–11.

18 P. Hu, X. Liu, B. Liu, L. Li, W. Qin, H. Yu, S. Zhong, Y. Li, Z. Ren and M. Wang, Hierarchical layered Ni3S2-graphene hybrid composites for efficient photocatalytic reduction of Cr(VI), *Journal of Colloid and Interface Science*, 2017, **496**, 254–260.

19 J. Yang, J. Hao, S. Xu, J. Dai, Y. Wang and X. Pang, Visible-light-driven photocatalytic degradation of 4-CP and the synergistic reduction of Cr(VI) on one-pot synthesized amorphous Nb2O5 nanorods/graphene heterostructured composites, *Chemical Engineering Journal*, 2018, **353**, 100–114.

20 J. Ye, J. Liu, Z. Huang, S. Wu, X. Dai, L. Zhang and L. Cui, Effect of reduced graphene oxide doping on photocatalytic reduction of Cr(VI) and photocatalytic oxidation of tetracycline by ZnAlTi layered double oxides under visible light, *Chemosphere*, 2019, **227**, 505–513.

21 P. Borthakur, M. R. Das, S. Szunerits and R. Boukherroub, CuS Decorated Functionalized Reduced Graphene Oxide: A Dual Responsive Nanozyme for Selective Detection and Photoreduction of Cr(VI) in an Aqueous Medium, *ACS Sustainable Chem. Eng.*, 2019, **7**, 16131–16143.

22 Y. Liu, D. Yang, T. Xu, Y. Shi, L. Song and Z.-Z. Yu, Continuous photocatalytic removal of chromium (VI) with structurally stable and porous Ag/Ag3PO4/reduced graphene oxide microspheres, *Chemical Engineering Journal*, 2020, **379**, 122200.

23 W. Liu, M. Wang, C. Xu and S. Chen, Facile synthesis of g-C3N4/ZnO composite with enhanced visible light photooxidation and photoreduction properties, *Chemical Engineering Journal*, 2012, **209**, 386–393.

24 G. Dong and L. Zhang, Synthesis and Enhanced Cr(VI) Photoreduction Property of Formate Anion Containing Graphitic Carbon Nitride, *J. Phys. Chem. C*, 2013, **117**, 4062–4068.

25 X. Hu, H. Ji, F. Chang and Y. Luo, Simultaneous photocatalytic Cr(VI) reduction and 2,4,6-TCP oxidation over g-C3N4 under visible light irradiation, *Catalysis Today*, 2014, **224**, 34–40.

26 Y. Zhang, Q. Zhang, Q. Shi, Z. Cai and Z. Yang, Acid-treated g-C3N4 with improved photocatalytic performance in the reduction of aqueous Cr(VI) under visible-light, *Separation and Purification Technology*, 2015, **142**, 251–257.

27 D. Xiao, K. Dai, Y. Qu, Y. Yin and H. Chen, Hydrothermal synthesis of α-Fe2O3/g-C3N4 composite

and its efficient photocatalytic reduction of Cr(VI) under visible light, *Applied Surface Science*, 2015, **358**, 181–187.

28 D. Lu, G. Zhang and Z. Wan, Visible-light-driven g-C3N4/Ti3+-TiO2 photocatalyst co-exposed {001} and {101} facets and its enhanced photocatalytic activities for organic pollutant degradation and Cr(VI) reduction, *Applied Surface Science*, 2015, **358**, 223–230.

29 H. Wei, Q. Zhang, Y. Zhang, Z. Yang, A. Zhu and D. D. Dionysiou, Enhancement of the Cr(VI) adsorption and photocatalytic reduction activity of g-C3N4 by hydrothermal treatment in HNO3 aqueous solution, *Applied Catalysis A: General*, 2016, **521**, 9–18.

30 R. Mohini and N. Lakshminarasimhan, Coupled semiconductor nanocomposite g-C3N4/TiO2 with enhanced visible light photocatalytic activity, *Materials Research Bulletin*, 2016, **76**, 370–375.

31 W. Huang, N. Liu, X. Zhang, M. Wu and L. Tang, Metal organic framework g-C3N4/MIL-53(Fe) heterojunctions with enhanced photocatalytic activity for Cr(VI) reduction under visible light, *Applied Surface Science*, 2017, **425**, 107–116.

32 Y. Zheng, Z. Yu, F. Lin, F. Guo, K. A. Alamry, L. A. Taib, A. M. Asiri and X. Wang, Sulfur-Doped Carbon Nitride Polymers for Photocatalytic Degradation of Organic Pollutant and Reduction of Cr(VI), *Molecules*, 2017, **22**, 572.

33 F. Liu, J. Yu, G. Tu, L. Qu, J. Xiao, Y. Liu, L. Wang, J. Lei and J. Zhang, Carbon nitride coupled Ti-SBA15 catalyst for visible-light-driven photocatalytic reduction of Cr (VI) and the synergistic oxidation of phenol, *Applied Catalysis B: Environmental*, 2017, **201**, 1–11.

34 Z. Wan, G. Zhang, X. Wu and S. Yin, Novel visible-light-driven Z-scheme Bi12GeO20/g-C3N4 photocatalyst: Oxygen-induced pathway of organic pollutants degradation and proton assisted electron transfer mechanism of Cr(VI) reduction, *Applied Catalysis B: Environmental*, 2017, **207**, 17–26.

35 J.-C. Wang, C.-X. Cui, Y. Li, L. Liu, Y.-P. Zhang and W. Shi, Porous Mn doped g-C3N4 photocatalysts for enhanced synergetic degradation under visible-light illumination, *Journal of Hazardous Materials*, 2017, **339**, 43–53.

36 Y. Yang, X.-A. Yang, D. Leng, S.-B. Wang and W.-B. Zhang, Fabrication of g-C3N4/SnS2/SnO2 nanocomposites for promoting photocatalytic reduction of aqueous Cr(VI) under visible light, *Chemical Engineering Journal*, 2018, **335**, 491–500.

37 S. Lamkhao, G. Rujijanagul and C. Randorn, Fabrication of g-C3N4 and a promising charcoal property towards enhanced chromium(VI) reduction and wastewater treatment under visible light, *Chemosphere*, 2018, **193**, 237–243.

38 Y. Deng, L. Tang, G. Zeng, Z. Zhu, M. Yan, Y. Zhou, J. Wang, Y. Liu and J. Wang, Insight into highly efficient simultaneous photocatalytic removal of Cr(VI) and 2,4-diclorophenol under visible light irradiation by phosphorus doped porous ultrathin g-C3N4 nanosheets from aqueous media: Performance and reaction mechanism, *Applied Catalysis B: Environmental*, 2017, **203**, 343–354.

39 S. Nayak and K. M. Parida, Dynamics of Charge-Transfer Behavior in a Plasmon-Induced Quasi-Type-II p–n/n–n Dual Heterojunction in Ag@Ag3PO4/g-C3N4/NiFe LDH Nanocomposites for

Photocatalytic Cr(VI) Reduction and Phenol Oxidation, *ACS Omega*, 2018, **3**, 7324–7343.

40 Y. Chang, Z. Liu, X. Shen, B. Zhu, D. K. Macharia, Z. Chen and L. Zhang, Synthesis of Au nanoparticle-decorated carbon nitride nanorods with plasmon-enhanced photoabsorption and photocatalytic activity for removing various pollutants from water, *Journal of Hazardous Materials*, 2018, **344**, 1188–1197.

41 X. Hu, W. Wang, G. Xie, H. Wang, X. Tan, Q. Jin, D. Zhou and Y. Zhao, Ternary assembly of g-C3N4/graphene oxide sheets /BiFeO3 heterojunction with enhanced photoreduction of Cr(VI) under visible-light irradiation, *Chemosphere*, 2019, **216**, 733–741.

42 C. Hu, Y.-C. Chu, Y.-R. Lin, H.-C. Yang and K.-H. Wang, Photocatalytic Dye and Cr(VI) Degradation Using a Metal-Free Polymeric g-C3N4 Synthesized from Solvent-Treated Urea, *Polymers*, 2019, **11**, 182.

43 H.-H. Wu, C.-W. Chang, D. Lu, K. Maeda and C. Hu, Synergistic Effect of Hydrochloric Acid and Phytic Acid Doping on Polyaniline-Coupled g-C3N4 Nanosheets for Photocatalytic Cr(VI) Reduction and Dye Degradation, *ACS Appl. Mater. Interfaces*, 2019, **11**, 35702–35712.

44 M. Ye, W. Wei, L. Zheng, Y. Liu, D. Wu, X. Gu and A. Wei, Enhanced visible light photoreduction of aqueous Cr(VI) by Ag/Bi4O7/g-C3N4 nanosheets ternary metal/non-metal Z-scheme heterojunction, *Journal of Hazardous Materials*, 2019, **365**, 674–683.

45 J. Zhang, N. Gao, F. Chen, T. Zhang, G. Zhang, D. Wang, X. Xie, D. Cai, X. Ma, L. Wu and Z. Wu, Improvement of Cr (VI) photoreduction under visible-light by g-C3N4 modified by nano-network structured palygorskite, *Chemical Engineering Journal*, 2019, **358**, 398–407.

46 X.-H. Yi, S.-Q. Ma, X.-D. Du, C. Zhao, H. Fu, P. Wang and C.-C. Wang, The facile fabrication of 2D/3D Z-scheme g-C3N4/UiO-66 heterojunction with enhanced photocatalytic Cr(VI) reduction performance under white light, *Chemical Engineering Journal*, 2019, **375**, 121944.

47 S. Kang, M. He, M. Chen, Y. Liu, Y. Wang, Y. Wang, M. Dong, X. Chang and L. Cui, Surface Amino Group Regulation and Structural Engineering of Graphitic Carbon Nitride with Enhanced Photocatalytic Activity by Ultrafast Ammonia Plasma Immersion Modification, *ACS Appl. Mater. Interfaces*, 2019, **11**, 14952–14959.

48 H. Wang, Q. Li, S. Zhang, Z. Chen, W. Wang, G. Zhao, L. Zhuang, B. Hu and X. Wang, Visible-light-driven N2-g-C3N4 as a highly stable and efficient photocatalyst for bisphenol A and Cr(VI) removal in binary systems, *Catalysis Today*, 2019, **335**, 110–116.

49 N. Zhang, G. Li, S. Wang, X. Xu and L. Li, TaCxOy: A photocatalytic promoter on g-C3N4 for visible-light Cr6+ reduction, *Catalysis Communications*, 2019, **119**, 129–133.

50 Q. Wang, P. Xu, G. Zhang, L. Hu and P. Wang, Visible-light responsive g-C3N4 coupled with ZnS nanoparticles via a rapid microwave route: Characterization and enhanced photocatalytic activity, *Applied Surface Science*, 2019, **488**, 360–369.

51 Q. Sun, X. Hu, S. Zheng, J. Zhang and J. Sheng, Effect of calcination on structure and photocatalytic property of N-TiO2/g-C3N4@diatomite hybrid photocatalyst for improving reduction of Cr(Ⅵ), *Environmental Pollution*, 2019, **245**, 53–62.

52 P. Babu, S. Mohanty, B. Naik and K. Parida, Serendipitous Assembly of Mixed Phase BiVO4 on B-Doped g-C3N4: An Appropriate p–n Heterojunction for Photocatalytic O2 evolution and Cr(VI) reduction, *Inorg. Chem.*, 2019, **58**, 12480–12491.
53 X. Wang, L. Li, J. Meng, P. Xia, Y. Yang and Y. Guo, Enhanced simulated sunlight photocatalytic reduction of an aqueous hexavalent chromium over hydroxyl-modified graphitic carbon nitride, *Applied Surface Science*, 2020, **506**, 144181.
54 Q. Meng, Y. Cai, B. Cong, W. Xing and G. Chen, Enhanced carriers separation efficiency in g-C3N4 modified with sulfonic groups for efficient photocatalytic Cr(VI) reduction, *Materials Research Bulletin*, 2020, **122**, 110681.
55 Q. Jin, G. Xie, X. Cai, X. Hu, H. Wang, G. Qiu, W. Wang, D. Zhou, H. Huo, X. Tan and Y. Zhao, Three-dimensional microspheric g-C3N4 coupled by Broussonetia papyrifera biochar: facile sodium alginate immobilization and excellent photocatalytic Cr(IV) reduction, *RSC Adv.*, 2020, **10**, 6121–6128.
56 R. Li, D. Hu, K. Hu, H. Deng, M. Zhang, A. Wang, R. Qiu and K. Yan, Coupling adsorption-photocatalytic reduction of Cr(VI) by metal-free N-doped carbon, *Science of The Total Environment*, 2020, **704**, 135284.